

Precise and accurate determination of the pK_w of heavy water via a new protocol within the Blue Moon ensemble: comparison to light water and implications for *ab initio* simulations

Daniel Muñoz-Santiburcio^{1, a)}

Instituto de Fusión Nuclear “Guillermo Velarde”, Universidad Politécnica de Madrid, C/ José Gutiérrez Abascal 2, 28006 Madrid, Spain

(Dated: 5 May 2024)

Water self-dissociation is one of the most studied reactions in aqueous medium, having received a special attention from the computational chemistry community. However, a precise and accurate *in silico* estimation of the pK_w remained elusive for a long time, until very recent works finally reached this goal with a strong technical effort. In this work, I define a very accessible procedure within the Blue Moon ensemble approach that allows a precise determination of the pK_w , correcting two effects present in the regular application of different constrained MD methods that caused a wrong description of the dissociated state. This approach, together with an extremely efficient *ab initio* setup within the Second-generation Car–Parrinello MD scheme, and a description of the electronic structure at the RPBE-D3 level, yields an estimation of the pK_w of heavy water that is practically equal to the experimental value. The comparison of this result with the one in light water provides interesting conclusions, with important implications for the *ab initio* simulation of water.

I. INTRODUCTION

Water self-dissociation is probably the most paradigmatic chemical reaction in aqueous medium, being responsible of the natural presence of H^+ and OH^- ions in pure water, and conditioning practically all the chemistry occurring in aqueous media (which includes the whole of biochemistry). Due to this tremendous importance, this reaction has been the subject of many computational studies along the last decades using different methods,^{1–9} especially free energy and enhanced sampling methods aimed at estimating the energetics of the reaction.

Because of the amphoteric character of water, finding a good reaction coordinate that correctly describes the full dissociation process has been a significant challenge. After the pioneering *ab initio* MD (AIMD) study of Trout and Parrinello,¹ it was quickly realized that the simplest reaction coordinate of the interatomic distance of a given O–H bond was not enough to accurately describe the dissociated state. This prompted Sprik to employ a O–H coordination number constraint,² which is a function of the interatomic distances between all the H atoms in the system and a specific oxygen atom. This coordinate greatly improved the description of the process, but it was noted that the free energy profile obtained from the integration of the corresponding forces of constraint did not show the appropriate local minimum at the dissociated state, indicating that the product state was still ill-defined.

In later works,^{3–5} it became clear that a correct description of the dissociated state requires considering not only the O–H coordination number of a given oxygen atom, but also the separation between the dissociation products $OH^-(aq)$ and $H_3O^+(aq)$. However, accounting

for the hydronium–hydroxide distance in a strict manner was complicated, since the location of the oxygen site of the hydronium was constantly changing due to its diffusion following the Grotthuss mechanism.^{10–12} This problem was solved by Grifoni *et al.*,¹³ who introduced two new generalized collective variables (CVs): the number of protonated/deprotonated species in the system and the distance between the formed ions (acid and base sites). These were defined employing a smooth Voronoi tessellation scheme which considers the positions of all hydrogen and oxygen atoms in the system, thus allowing for the free structural diffusion of both $OH^-(aq)$ and $H_3O^+(aq)$.

Thanks to the introduction of such generalized coordinates, three recent works have shown remarkably detailed descriptions of the self-dissociation process, reaching very precise estimations of its energetics. In the first one, Joutsuka performed a thorough AIMD study⁶ at the revPBE-D3 level employing umbrella sampling with two CVs to describe the reaction in a 256 H_2O system. While one of these CVs was the hydronium–hydroxide distance as proposed by Grifoni *et al.*,¹³ the other was the usual O–H coordination number defined for a specific oxygen site. With that procedure, that work was the first to obtain a 2D free energy surface (FES) for the self-dissociation reaction where the local minimum belonging to the product state could be identified, estimating the pK_w at 298 K as 13.7. This value corresponds to a free energy difference between the neutral and dissociated states of 78.2 kJ/mol, in very good agreement with the experimental value of 79.9 kJ/mol at 298 K.^{14,15}

In the second of these studies,⁷ Liu *et al.* carried out rather cumbersome metadynamics simulations with 2 CVs, employing machine learning (ML) methods, in particular neural network potentials (NNPs) trained at the RPBE-D3 level. The CVs used were the generalized hydronium–hydroxide distance defined earlier¹³ and a generalized number of ions with a different functional

^{a)}Electronic mail: daniel.munozsan@upm.es

form compared to the one defined by Grifoni *et al*, but which still allows the formed OH^- (aq) ion (in addition to the H_3O^+ (aq)) to freely diffuse along the different water molecules in the system, which was not possible in the previous works that used the regular O–H coordination number constraint.^{2–4,6,9} In this way, the authors were able to describe quite thoroughly the energetic landscape of the dissociation/recombination reactions, simulating systems of different sizes from 64 to 512 H_2O molecules. By analyzing the reconstructed FES, they found a free energy difference between reactants and products of 77.3 kJ/mol, equivalent to a $\text{p}K_{\text{w}}$ of 13.55 at 298 K. However, the standard ML potential used did not account for the electrostatic energy necessary to separate the formed OH^- (aq) and H_3O^+ (aq) ions. Thus, the authors introduced an electrostatic correction and employed the rate constants of the elementary reaction steps to estimate a final value of $\text{p}K_{\text{w}} = 14.14$ (which translates into $\Delta F = 80.7$ kJ/mol).

Finally, in the most recent work Calegari *et al*⁸ performed metadynamics simulations with a ML potential which included the long range electrostatic interactions, since it was also trained to reproduce the Wannier centroids of the system,¹⁶ employing the SCAN functional for the training.¹⁷ In addition, they performed analogous metadynamics simulations with a regular ML potential which did not include the long range electrostatics, in order to check the extent to which these interactions affect the estimated $\text{p}K_{\text{w}}$. In contrast with the two previous works, here the metadynamics simulations employed only one CV, namely the hydronium-hydroxide distance,¹³ together with a restraint to allow for only one dissociated water molecule in the system. The authors also determined the size dependence of the estimated dissociation free energy, reaching system sizes of up to 1024 H_2O molecules, finding that at least 500 molecules are needed to converge the dissociation free energy with respect to the system size. In particular, they found a $\text{p}K_{\text{w}}$ of 14.7 for water at ~ 293 K (equivalent to $\Delta F = 82.5$ kJ/mol, in comparison to the experimental 79.5 kJ/mol at that T¹⁴) when including the long range electrostatic effects, in comparison to a $\text{p}K_{\text{w}}$ value of 10.7 (i.e. $\Delta F \sim 60$ kJ/mol) when not considering them. It is noted in passing that the simulation temperature was 330 K in order to correct for a well-known overestimation of the H-bond strength produced by SCAN, providing a water dynamics corresponding to the experimental one at ~ 293 K.

Despite these three recent studies^{6–8} have greatly improved the existing procedures for computationally estimating the $\text{p}K_{\text{w}}$, applying these in a routine fashion (e.g. to investigate the change of $\text{p}K_{\text{w}}$ at several different conditions and environments, such as bulk *vs.* nanoconfinement^{3,4,9}) is still remarkably challenging. In particular, these three works required reaching large size scales in order to obtain a proper description of the dissociated state, plus very long timescales in order to obtain the required statistics. While in Ref. 6, the necessary time and size scales were reached by sheer computational effort

performing strict AIMD simulations, in Refs. 7,8 they reached even larger simulation times and sizes thanks to the use of ML methods. However, ML methods are rather non-trivial to use as they require a careful training procedure, which also involves carrying out many calculations at the *ab initio* level of theory.

Therefore, it would still be very convenient to have a protocol for estimating the ΔF of the water self-dissociation reaction, but without the need of huge system sizes and with the simplest possible free energy method, so that the whole study can be carried out at the *ab initio* level. In this paper, I propose a new procedure within the framework of the Blue Moon ensemble approach that allows to estimate the $\text{p}K_{\text{w}}$ in an univocal and precise way within the underlying level of theory. This procedure requires only a few (on the order of 3–5) additional simulation replica compared to the regular application of the method, using the same O–H coordination number constraint, and thus with a smaller computational cost compared to using a second CV. As I will expose in the following sections, in the first place I carefully defined this procedure for bulk light water, and later applied it again to estimate the $\text{p}K_{\text{w}}$ of bulk heavy water, in both cases at the RPBE-D3 level of theory. Anticipating the key results, the comparison of both estimations with the corresponding experimental values provides important insights about to what extent the error cancellations when using GGA functionals with classical nuclei compensates for the missing nuclear quantum effects in water.

II. METHODS

A. General AIMD settings

In a previous study¹⁸ I carried out an extensive technical work in order to set up the very efficient Second-generation Car–Parrinello MD method (2nd-gen. CPMD) for simulating neutral, acidic and basic liquid water. There, I showed that a careful setup produces a propagation regime that is in practice indistinguishable from that in the Born–Oppenheimer limit. This removed the need for employing a Langevin dynamics propagation scheme as used in the original formulation of the 2nd-gen. CPMD method,^{19,20} thus being possible to employ it in conjunction with any regular thermostat such as Nosé–Hoover chains or CSVR,²¹ which are much more efficient for obtaining a canonical sampling than the Langevin dynamics scheme. Moreover, the results for neutral, acidic and basic water showed that the employed level of theory provided a remarkably good estimation of the diffusion coefficients of H_2O and the excess proton and hydroxide ions in bulk water, which strongly supports its use for studying the water self-dissociation reaction.

In consequence, in this work I rely on the settings defined in Ref. 18, which I summarize in the following. All the simulations were carried out with CP2K.²² The

model system for neutral light water consisted in 128 H₂O molecules in a cubic cell with $L = 15.663$ Å, corresponding to a water density of 996.556 kg/m³, which matches the experimental value at $T = 300$ K and $p = 1$ bar.²³ Additional simulations were carried out for an equivalent basic light water system (obtained by removing a proton from the previous simulation cell); and also for a neutral light water system in a bigger simulation cell in order to check the presence of finite size effects, employing 256 H₂O molecules in a cubic cell with $L = 19.734$ Å. Finally, further simulations carried out to study the self-dissociation of heavy water used the same cell size as before, thus taking 128 D₂O molecules in a $L = 15.663$ Å cubic cell (again removing a proton for getting the equivalent basic heavy water system).

As in Ref. 18, I employed the spin-restricted Kohn-Sham formulation with the RPBE functional²⁴ together with D3 corrections²⁵ (which included only the two-body terms and zero damping), using GTH pseudopotentials^{26–28} and a TZV2P basis set.²⁹ I employed a 500 Ry density cutoff for the expansion of the auxiliary planewave basis set, with NN50 smoothing for both the charge density and its derivatives. I refer to Ref. 18 for further information on the computational approach, including careful tests demonstrating that the TZV2P basis set provides the best accuracy/cost relationship for the atomic forces of water containing excess proton and hydroxide ions (providing better accuracy than the popular DZVP-MOLOPT-SR basis set, and much better accuracy than the TZVP basis set).

With these electronic structure settings, I carried out AIMD simulations³⁰ using the Second-generation Car-Parrinello MD method^{19,20} with a 0.4 fs timestep, taking a fixed number of two corrector steps per AIMD step and an order of 2 for the ASPC extrapolation. In order to obtain a canonical sampling, I used the Nosé–Hoover chains thermostat with a target temperature of 300 K, a chain length of 3, an order of 9 for the Yoshida integrator, and a time constant of 100 fs.

B. Blue Moon ensemble settings

The initial purpose of this work was to devise a corrected version of the Blue Moon ensemble method that allows an univocal determination of the free energy barrier of the water-self dissociation reaction. The Blue Moon method^{31,32} consists in carrying out a set of constrained MD simulations, where a certain collective variable ξ is used as a reaction coordinate that drives the process of interest. In each simulation replica, this collective variable is constrained to a certain value ξ' , and the average force of constraint in that case is given by

$$\langle f_{\xi'} \rangle = \frac{\langle Z^{-1/2} [\lambda - k_B T G] \rangle_{\xi'}}{\langle Z^{-1/2} \rangle_{\xi'}} \quad (1)$$

where λ is the Lagrange multiplier associated to the constraint at each MD step, k_B is the Boltzmann constant,

T is the simulation temperature, and the weight factor Z and the correction term G are defined as

$$Z = \sum_i^N \frac{1}{m_i} \left(\frac{\partial \xi}{\partial \mathbf{r}_i} \right)^2 \quad (2)$$

$$G = \frac{1}{Z^2} \sum_{i,j}^N \frac{1}{m_i m_j} \frac{\partial \xi}{\partial \mathbf{r}_i} \frac{\partial^2 \xi}{\partial \mathbf{r}_i \partial \mathbf{r}_j} \frac{\partial \xi}{\partial \mathbf{r}_j} \quad (3)$$

where i, j run over all atoms in the system.

Once the set of $\langle f_{\xi'} \rangle$ values has been computed, the free energy change of the system between the states A and B can be straightforwardly computed as

$$\Delta F_{A \rightarrow B} = F(\xi_B) - F(\xi_A) = - \int_{\xi_A}^{\xi_B} \langle f_{\xi} \rangle d\xi \quad (4)$$

I note in passing that sometimes, the average forces of constraint are assumed to be equal to the averages of the Lagrange multipliers (i.e. $\langle f_{\xi'} \rangle = \langle \lambda \rangle_{\xi'}$), which is not strictly true except for specific, simple constraints such as the distance between two given atoms (in which case $Z = 1$ and $G = 0$).

The reaction coordinate chosen for driving the self-dissociation reaction in this work is the coordination number n of a specific oxygen atom O* with respect to all hydrogen atoms (or deuterium in the case of heavy water), with the functional form

$$n = \sum_i \frac{1 - \left(\frac{r_{O^*H_i}}{r_0} \right)^a}{1 - \left(\frac{r_{O^*H_i}}{r_0} \right)^b} \quad (5)$$

where i runs over all H atoms in the system, $r_{O^*H_i}$ is the distance between atoms O* and H_{*i*}, $r_0 = 1.44183$ Å, $a = 10$ and $b = 28$. These values of r_0 , a and b were chosen so that the shape of n as a function of $r_{O^*H_i}$ reproduces the shape of the coordination number used in Refs. 2,3. In all cases, I will denote the average forces of the coordination number constraint on the different simulation replica as $\langle f_n \rangle$, always computed following Eqs. 1–3.

In the regular application of the Blue Moon method for water self-dissociation, all the simulation replica correspond to a neutral water system, which I generated as follows: in a well equilibrated system taken from the simulations presented in Ref. 18, I chose a random oxygen atom as O* and introduced the coordination number constraint n with an initial value coincident with that in such initial state, which happened to be $n \sim 2$ as expected for a neutral water molecule. Then, I carried out a simulation where the constraint was forced to slowly decrease until $n \sim 1$, so that the system remained in equilibrium at all times. During this simulation, I collected the particle positions, velocities, and thermostat information at specific values of n , which were used as initial conditions for the different simulation replica. Each of these replica, where n was constrained to a fixed value, was equilibrated

for at least 5 ps, and followed by 190 ps of production run (except a few specific replica where I reached 220 ps of total production time, see caption of Fig. 2).

As will be explained below, the protocol developed in this work also involved different replica in a basic light water system, which were generated as in the neutral water case, except for the fact that the O^* atom was not randomly chosen but obviously set to be the O site of the OH^- ion at the initial step. As in the neutral water case, the initial conditions for the different replica were generated during a simulation with a slowly changing constraint, then equilibrated for 5 ps and continued during 190 ps of production time.

The replica for the neutral and basic heavy water systems were generated with the same procedure as above, with the ‘slowly changing constraint’ simulations starting from regular (i.e. unconstrained) neutral and basic heavy water systems previously equilibrated for 10 ps. Again, every individual replica was further equilibrated for 5 ps, followed by 190 ps of production run.

In order to obtain a high accuracy in the estimation of ΔF , I employed a notably big amount of simulation replica, with a especially fine discretization of n in the regions where the average forces of constraint $\langle f_n \rangle$ would change significantly when varying n . In particular, the final estimations of ΔF provided in Sec. III C required at least 30 replica for each of the light and heavy water systems (in each case, at least 27 replica for the neutral system, and 3 for the basic system).

Finally, I note that in the rest of this paper I will be referring to the solvated self-dissociation products as OH^- and H_3O^+ , omitting the ‘(aq)’ for the sake of readability.

III. RESULTS AND DISCUSSION

A. Limitations of the regular approach

In Fig. 1 I show the free energy profile of the H_2O self-dissociation reaction directly obtained by the regular application of the Blue Moon ensemble method (i.e. integration of the average forces of constraint obtained for the different simulation replica, Eq. 4). As in several studies using a coordination number constraint,^{2-4,6,9} the ΔF profile presents a hooked shape at the dissociated state with no hint of a local minimum at all, with ΔF evolving from being linear in the region $1.25 < n < 1.5$ to convex for $n < 1.25$. This convexity appears due to the increasing average forces of constraint as we approach the dissociated state, in stark contrast to the expectation that $\langle f_n \rangle$ should become 0 at some point when $n \rightarrow 1$, so that the integration of $\langle f_n \rangle$ would produce a maximum or plateau in that region.

Clearly, the regular computational protocol was not reproducing the correct qualitative behavior of the energetics of the reaction at the dissociated state. In order to confirm the reasons of this failure, I began by inspecting

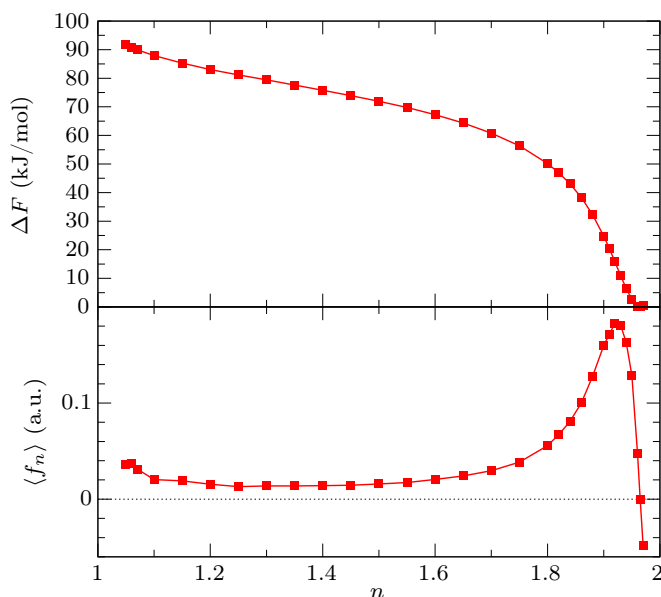


FIG. 1. Free energy profile ΔF (top panel) for the self-dissociation of H_2O relative to the reactant state directly obtained from the usual application of the Blue Moon ensemble method, i.e. integrating the average forces of constraint $\langle f_n \rangle$ (bottom panel) obtained from the different simulation replica with different values of the constraint n .³³

in detail what is the *in silico* description of the dissociated state produced by this protocol.

Analysis of the different trajectories shows that the water molecule becomes indeed dissociated as $n \rightarrow 1.1$, the difference among the different replica being the arrangement and behavior of the formed H_3O^+ ion with respect to the OH^- . As seen in Figs. 2 and 3, for $n = 1.35$ and 1.3 the H_3O^+ is practically the whole time coordinated to the OH^- , with occasional very short diffusion events (‘proton rattling’) to its second solvation shell. In the region $1.15 \leq n \leq 1.25$, the H_3O^+ occasionally diffuses farther from the second OH^- solvation shell, and for $n = 1.1$ it becomes fully free, diffusing via the Grotthuss mechanism through the whole liquid phase, though still with very frequent encounters with the OH^- due to the small system size. While there is the reasonable doubt of whether the H_3O^+ is already fully free already at some point between $n = 1.25$ and 1.15 , it must be recognized that the ‘excursions’ of the hydronium beyond the second solvation shell of the hydroxide are rather short, and moreover the probability distributions of the distance $d(O^* - O_a)$ (where O_a denotes the oxygen atom of the formed H_3O^+) do not show a real qualitative change until $n = 1.1$, which is the first value as n decreases where the probability of finding the excess proton out of the first solvation shell of the OH^- is greater than within it (bottom panel of Fig. 3). This is also confirmed by analyzing the radial distribution functions $g_{O^*H}(r)$ and $g_{O^*O}(r)$ in Fig. 4, where for $n = 1.15$ the peak corresponding to the dissociating proton is still evident and distinct from the one belonging to

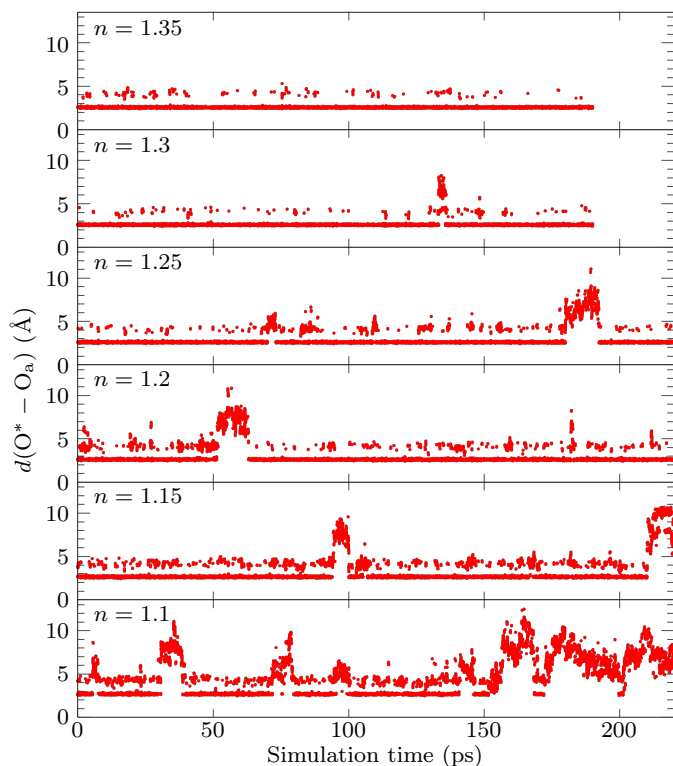


FIG. 2. Time evolution of the distance between the oxygen atom where the formed OH^- ion is pinned (O^*) and the oxygen atom of the formed H_3O^+ (O_a), for the constraint values in the range $1.1 \leq n \leq 1.35$. Note that the replica with $1.1 \leq n \leq 1.25$ were sampled until $t = 220$ ps (and not 190 ps like the other cases) in order to improve the statistics around the dissociated state.

the donor hydrogen bonds of the solvating waters, while at $n = 1.1$ there is only one peak qualitatively equal to that in a regular OH^- solvation shell. Finally, I remark again that the employed reaction coordinate n prohibits the diffusion of the formed OH^- at the dissociated state, since it prevents the O^* atom with which it was defined from receiving not only the H atom that has dissociated from it, but *any* H atom in the system.

Having checked the *in silico* description of the dissociated state, I now compare it to the actual experimental reality. I recall that the well-known experimental value of $\text{p}K_w = 14$ at ambient conditions translates into a molal concentration of free H^+ and OH^- ions of 10^{-7} mol/kg, which means that on average there is a pair of free H^+ and OH^- ions for every 5.55×10^8 water molecules in the bulk. This implies that, while in nature the H_3O^+ and OH^- ions resulting from water self-dissociation are most of the time freely diffusing across water's H-bond network, and only seldomly encountering each other, the current computational protocol is modeling the dissociated state as a $\text{OH}^-/\text{H}_3\text{O}^+$ ion pair that suffers very frequent recombinations due to the small cell size (a size effect that has been abundantly recognized⁶⁻⁸), and where moreover the OH^- ion is *not* diffusing at all because of the very con-

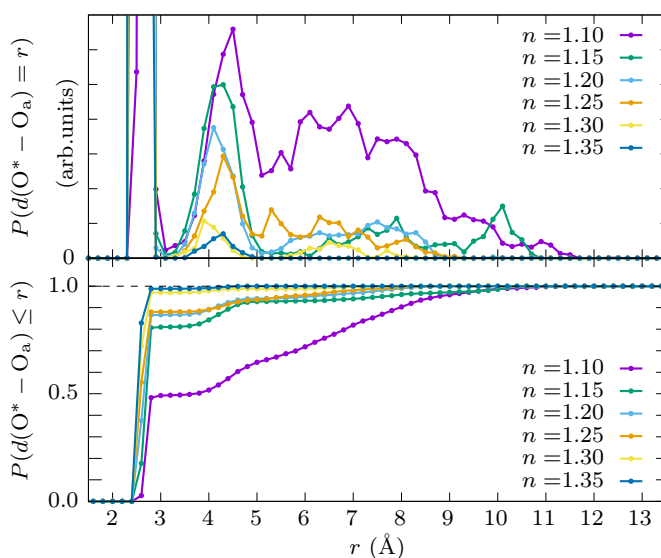


FIG. 3. Normalized distribution (top panel) and accumulated distribution (bottom panel) of the probability of finding the oxygen of the formed H_3O^+ (O_a) at or below a certain distance r from the oxygen site where the OH^- ion is pinned (O^*), for the constraint values in the range $1.1 \leq n \leq 1.35$.

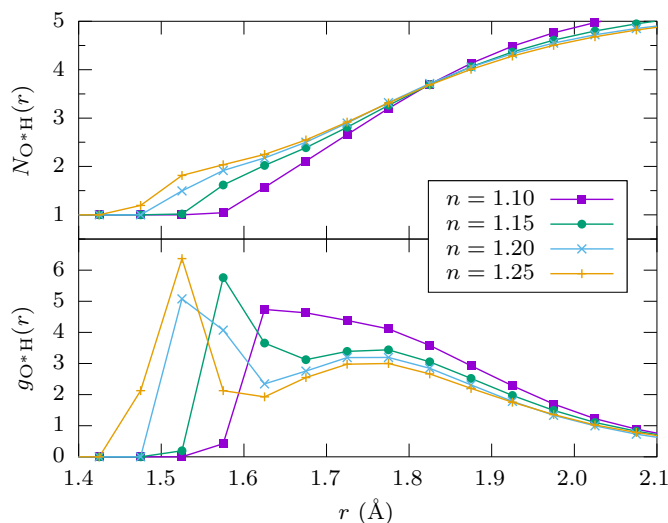


FIG. 4. Radial distribution function $g_{\text{O}^*\text{H}}(r)$ (bottom panel) and running coordination number $N_{\text{O}^*\text{H}}(r) = \int_0^r g_{\text{O}^*\text{H}}(r') dr'$ (top panel; do not confuse with the coordination number constraint n) magnified in the region where the H-bonds accepted by the OH^- ion show up for different values of the coordination number constraint n .

straint that is used to drive the dissociation of a precise water molecule. Obviously, each of these facts has an associated energetic cost, which we should remove in order to recover the correct ΔF profile.

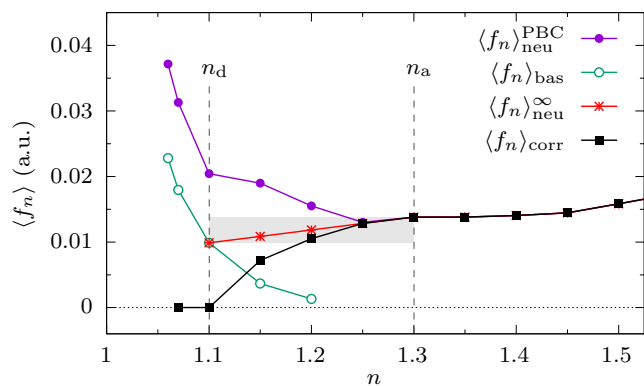


FIG. 5. Average forces of constraint directly obtained from the regular application of the Blue Moon ensemble method (Eqs. 1–3) on the finite-size neutral water system, $\langle f_n \rangle_{\text{neu}}^{\text{PBC}}$, together with the equivalent average forces of constraint for a basic water system $\langle f_n \rangle_{\text{bas}}$, the estimated average forces of constraint for an infinite neutral water system $\langle f_n \rangle_{\text{neu}}^{\infty}$ (with the associated uncertainty region shaded in grey), and the final corrected estimation of the average forces of constraint $\langle f_n \rangle_{\text{corr}}$. See text for details.

B. Recovering the correct ΔF profile

I begin by analyzing the effect of ‘pinning’ the formed OH^- on a precise oxygen site, which has been so far ignored in the literature until the present work. The previous reflection on the concentration of $\text{H}_3\text{O}^+/\text{OH}^-$ ions in ambient bulk water shows that the OH^- arising from a dissociated H_2O is most of the time locally indistinguishable from a free OH^- in a basic solution. This immediately suggests that the ‘pinning’ effect should be clearly visible in a set of simulations of a *basic* water system (i.e. containing a single OH^- plus N neutral H_2O molecules) where the OH^- is localized on a given oxygen site O^* by using the same coordination number constraint n as previously used in the globally neutral water system.

In Fig. 5, I show the average forces of constraint obtained earlier for the neutral system $\langle f_n \rangle_{\text{neu}}^{\text{PBC}}$ in the region around the dissociated state, together with the average forces of constraint obtained for the basic system $\langle f_n \rangle_{\text{bas}}$. The ‘PBC’ superscript present in the former, but not in the latter, makes it clear that the average forces of constraint in the neutral system are dependent on the system size due to the ‘recombination stress’ imposed by the free H_3O^+ being jailed in such small simulation cell together with the OH^- , while in the case of the basic system the cell size is irrelevant (as long as it allows the correct solvation structure of the OH^- , which is for sure granted with the present system size).

From Fig. 5 it is immediately evident that the localization of the OH^- imposed by the constraint has an energetic cost that increases as $n \rightarrow 1$. Actually, both $\langle f_n \rangle_{\text{neu}}^{\text{PBC}}$ and $\langle f_n \rangle_{\text{bas}}$ present practically the same convexity when $n \rightarrow 1$, further confirming that this energetic penalty was embedded into the ΔF profile obtained in

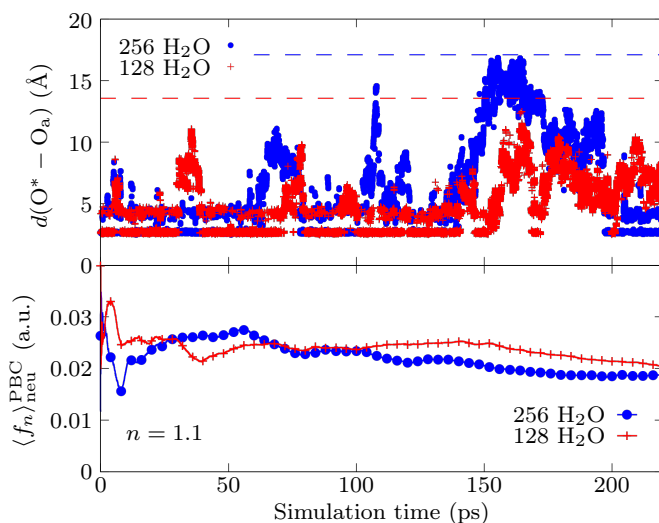


FIG. 6. Top panel: time evolution of the distance between the oxygen atom of the formed OH^- ion (O^*) and the oxygen atom of the formed H_3O^+ (O_a), for a constraint value of $n = 1.1$ in two liquid systems with 256 and 128 H_2O molecules. The dashed blue (resp. red) line indicates the maximum possible value for $d(\text{O}^* - \text{O}_a)$ due to the periodic boundary conditions in the 256 (resp. 128) H_2O system, which for a cubic unit cell is equal to $L\sqrt{3}/2$. Bottom panel: evolution of the average force of constraint for $n = 1.1$ in the 256 and 128 H_2O systems.

the regular approach. I also note that in this case $\langle f_n \rangle_{\text{bas}}$ becomes negative for $n \geq 1.25$ (not shown in Fig. 5 for simplicity), which means that it does no longer account for the energetic penalty of pinning the OH^- , but instead accounts for the energy gain of the OH^- when allowed to receive a proton from the solvating waters.

Now, we must determine the energetic cost associated to the finite-size effect arising from the frequent recombinations of the free H_3O^+ and the localized OH^- . A try to estimate this contribution performing a test simulation corresponding to the dissociated state in a bigger system, with 256 H_2O molecules, is shown in Fig. 6. As clearly seen there, converging the $\langle f_n \rangle_{\text{neu}}^{\text{PBC}}$ in that way would require much longer timescales than the 220 ps used there and an even bigger system, in agreement with the recent study of Calegari *et al.*⁸

This realization seems discouraging when trying to determine the correct ΔF profile in a computationally affordable way. However, carefully considering all the previous information, it is still possible to define a procedure that allows a cheap and well-grounded univocal estimation of ΔF . I start by assuming that, for the employed coordination number constraint n (Eq. 5), there exists a set of average forces of constraint for the self-dissociation of a H_2O molecule in the limit of an infinite system size and infinite sampling time, $\langle f_n \rangle_{\text{neu}}^{\infty}$. Obviously, such values would be free of any finite size effect by construction, but still they would include the energetic penalty due to the forbidden OH^- diffusion, which is intrinsic to the

constraint n used. However, this penalty can be estimated by computing the average forces of constraint in a bulk *basic* water system, $\langle f_n \rangle_{\text{bas}}$, which as I exposed earlier are not dependent on the system size. Therefore, if $\langle f_n \rangle_{\text{neu}}^\infty$ were known, the correct (or corrected) set of average forces of constraint devoid of both the localization and the size-dependent ‘recombination stress’ effects would be given by

$$\langle f_n \rangle_{\text{corr}} = \langle f_n \rangle_{\text{neu}}^\infty - \langle f_n \rangle_{\text{bas}} \quad (6)$$

where, as discussed above, $\langle f_n \rangle_{\text{bas}}$ is considered defined only for those n values in the neighborhood of the dissociated state that fulfill $\langle f_n \rangle_{\text{bas}} > 0$ (otherwise considering it as 0 in Eq. 6).

Thus, the problem is now reduced to finding $\langle f_n \rangle_{\text{neu}}^\infty$ for the different values of n . As exposed above, while a direct estimation of the finite-size effect is computationally cumbersome, it is easy to reconstruct $\langle f_n \rangle_{\text{neu}}^\infty$ if we realize that it must satisfy certain boundary conditions:

i) It is clear from the previous discussion that in the limit of an infinite system, once the reaction is finished, the formed OH^- must be indistinguishable from any hydroxide ion in a dilute basic solution. This implies that

$$\langle f_{n_d} \rangle_{\text{neu}}^\infty = \langle f_{n_d} \rangle_{\text{bas}} \quad (7)$$

being n_d the constraint value at which the dissociation reaction is completed. In the current case, I consider $n_d = 1.1$, according to the analysis exposed in Sec. III A.

ii) For the first stages of the dissociation reaction, while the nascent proton has not yet left its initial oxygen site, the system-size effect does not exist since the forces of constraint depend only on the very local solvation environment around the H_2O to be dissociated. This also applies to the stages where the OH^- and H_3O^+ exist as an associated pair, i.e. where the H_3O^+ can not diffuse farther away from the first solvation shell of the hydroxide (noting that some occasional proton rattling out of this first OH^- solvation does not constitute actual structural diffusion). Therefore,

$$\langle f_n \rangle_{\text{neu}}^\infty = \langle f_n \rangle_{\text{neu}}^{\text{PBC}} \quad \forall n \geq n_a \quad (8)$$

being n_a the smallest constraint value at which the OH^- does not diffuse farther away from the first OH^- solvation shell. In the present case, we can take $n_a = 1.3$, noting that the diffusion event at $t \sim 135$ ps seen in Fig. 2 for this simulation replica seems more a rattling event than actual structural diffusion.

iii) Finally, we must estimate $\langle f_n \rangle_{\text{neu}}^\infty$ for $n_d < n < n_a$, which in our case corresponds to the region $1.1 < n < 1.3$. In this stage, the hydronium is capable of diffusing farther from the first solvation shell of the hydroxide, but not yet far enough to avoid a fast recombination. Different works point out that this may occur at least until the H_3O^+ and OH^- are at the ends of a 4-molecule water wire,³⁴ or while their separation is at least 8 Å or possibly larger,⁸ for which an affordable 128 H_2O box as used here (with $L/2 = 7.8$ Å) is insufficient.

Therefore, while the computed value $\langle f_n \rangle_{\text{neu}}^{\text{PBC}}$ in this region is not helpful, we can still make a very reasonable guess for $\langle f_n \rangle_{\text{neu}}^\infty$ thanks to the conditions *i* and *ii* above. Looking at Fig. 5, and considering that $\langle f_{n_d} \rangle_{\text{neu}}^\infty = \langle f_{n_d} \rangle_{\text{bas}}$ and $\langle f_{n_a} \rangle_{\text{neu}}^\infty = \langle f_{n_a} \rangle_{\text{neu}}^{\text{PBC}}$, it seems obvious to expect that

$$\langle f_{n_d} \rangle_{\text{neu}}^\infty < \langle f_n \rangle_{\text{neu}}^\infty < \langle f_{n_a} \rangle_{\text{neu}}^\infty \quad \forall n_d < n < n_a \quad (9)$$

i.e. $\langle f_n \rangle_{\text{neu}}^\infty$ must lie in the shaded rectangular region in Fig. 5. Given that this region is quite narrow, it is safe to estimate $\langle f_n \rangle_{\text{neu}}^\infty$ as the diagonal of that rectangle

$$\langle f_n \rangle_{\text{neu}}^\infty = \langle f_{n_d} \rangle_{\text{bas}} + (n - n_d) \frac{\langle f_{n_a} \rangle_{\text{neu}}^{\text{PBC}} - \langle f_{n_d} \rangle_{\text{bas}}}{n_a - n_d} \quad (10)$$

$$\forall n_d < n < n_a$$

with the associated error being \pm half the rectangle area, i.e. $\pm(n_a - n_d)(\langle f_{n_a} \rangle_{\text{neu}}^{\text{PBC}} - \langle f_{n_d} \rangle_{\text{bas}})/2$.

Taking into account all the previous information, the definition in Eq. 6 and the conditions in Eqs. 7–10, the corrected averages of the force of constraint are given by

$$\langle f_n \rangle_{\text{corr}} = \quad (11)$$

$$= \begin{cases} 0 & \text{if } n \leq n_d \\ \langle f_{n_d} \rangle_{\text{bas}} + (n - n_d) \frac{\langle f_{n_a} \rangle_{\text{neu}}^{\text{PBC}} - \langle f_{n_d} \rangle_{\text{bas}}}{n_a - n_d} & \text{if } n_d < n < n_a \\ \langle f_n \rangle_{\text{neu}}^{\text{PBC}} & \text{if } n \geq n_a \end{cases}$$

where n_d and n_a have been defined earlier, and as said above $\langle f_n \rangle_{\text{bas}}$ is defined only for the few replica around n_d which fulfill $\langle f_n \rangle_{\text{bas}} > 0$ (being 0 otherwise).

Finally, I note that this proposed functional form will produce a plateau at the dissociated state, which implies that the free energy difference between the product and the transition state is negligible, i.e. that the recombination of the OH^- and H_3O^+ ions is barrierless. This assumption, which is implicit in the derivation of Eq. 11, is in line with the results of studies on the OH^- and H_3O^+ recombination employing unbiased AIMD simulations,³⁴ as well as with the shape of the free energy profile obtained by Calegari *et al.*⁸

C. Univocal estimation of the pK_w of light and heavy water

Having defined the procedure to get the correct average forces of constraint $\langle f_n \rangle_{\text{corr}}$ for the water self-dissociation reaction, it is straightforward to apply Eq. 4 to compute the corresponding free energy barrier for light water (Fig. 7). The result is $\Delta F_{\text{H}_2\text{O}}^{\text{sim}} = 84.3 \pm 1.0$ kJ/mol, which is ~ 4 kJ/mol larger than the corresponding experimental value at 300 K, $\Delta F_{\text{H}_2\text{O}}^{\text{exp}} = 80.0$ kJ/mol.^{14,15}

The offset of the present simulation result w.r.t. the experimental value may seem slightly disappointing in view of the results of Refs. 6, 7 and 8, which are closer to the experiment. However, it happens that the $\Delta F_{\text{H}_2\text{O}}^{\text{sim}}$ obtained here is actually almost equal to the experimental value for *heavy* water, $\Delta F_{\text{D}_2\text{O}}^{\text{exp}} = 85.5$ kJ/mol.^{35,36}

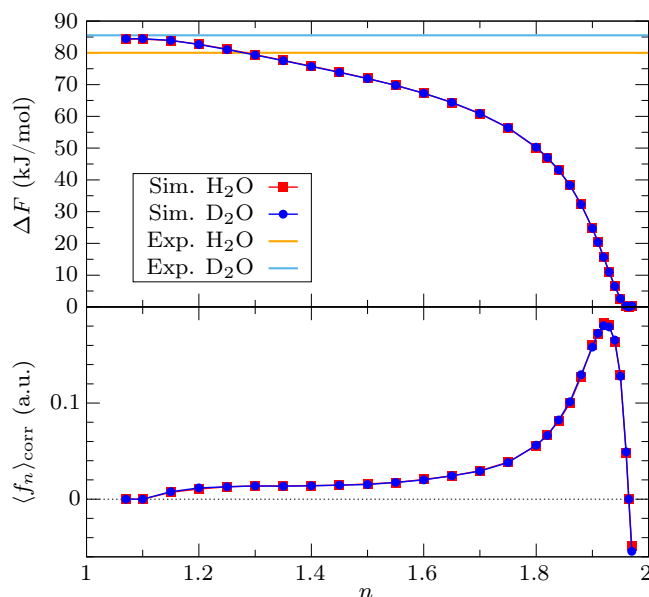


FIG. 7. Free energy profile ΔF (top panel) for the self-dissociation of H_2O and D_2O relative to the reactant state obtained from the procedure explained in this work, i.e. integrating the corrected average forces of constraint $\langle f_n \rangle_{\text{corr}}$ (bottom panel).

This makes a considerable sense, given that the employed computational approach considers all atomic nuclei as classical particles, thus not explicitly including different nuclear quantum effects (NQEs) such as the zero-point energy (ZPE), which is usually pointed out as the reason for the greater $\text{p}K_{\text{w}}$ of D_2O compared to H_2O .³⁶

This raises the question of what would be the simulation result if we repeat the same protocol for D_2O : would we obtain the same result as for light water, given the absence of NQEs in both simulation sets, or would we find some difference arising from classical effects due to the different H *vs.* D mass? To answer that question, I performed another set of constrained AIMD simulations employing heavy water, with the same computational settings and protocol previously used for light water. Not surprisingly, the simulation results of both light and heavy water are in practice identical (Fig. 7), with $\Delta F_{\text{D}_2\text{O}}^{\text{sim}} = 84.4 \pm 0.9$ kJ/mol. I note in passing that the convergence of these values is excellent, as seen in Fig. 8. Actually, this procedure performs extremely well even with relatively short simulation times, since only ~ 30 ps of simulation time for each replica are enough to obtain a ΔF^{sim} within ± 0.5 kJ/mol of the converged value.

D. Discussion and comparison with recent results in the literature

This double coincidence (i.e. $\Delta F_{\text{H}_2\text{O}}^{\text{sim}} = \Delta F_{\text{D}_2\text{O}}^{\text{sim}} \cong \Delta F_{\text{D}_2\text{O}}^{\text{exp}}$) has important implications. In the first place, it

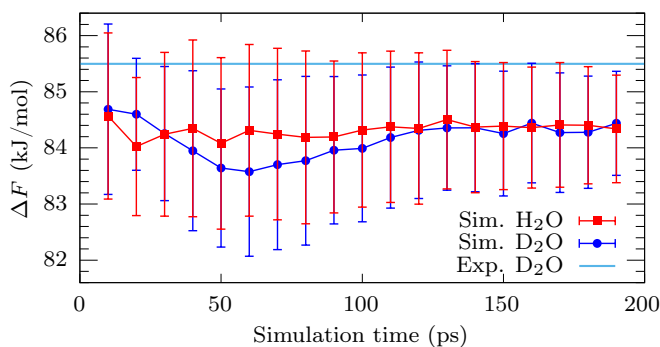


FIG. 8. Convergence w.r.t. simulation time of the computed values for the free energy barrier of the self-dissociation reaction with its corresponding error bars for light and heavy water, in comparison to the experimental value for heavy water.

confirms that in the self-dissociation of light and heavy water there are no classical effects at all arising from the different H/D masses. In second place and most importantly, I recall that usually the good qualitative and quantitative results obtained in simulations of water with regular GGA functionals (with or without dispersion corrections) when using classical nuclei are said to be due to the cancellation of the errors intrinsic to the GGA (usually the lack of self-interaction) and the missing NQEs.³⁷ Thus, the present D_2O simulation result being practically equal to the experimental value implies that the error compensation intrinsic to the level of theory used in this work (i.e. the RPBE-D3 functional with all the associated technical settings such as basis sets, pseudopotentials, etc.) accounts for the missing NQEs to an extent which is almost equal to the NQEs present in heavy water. Indeed, it must be recognized that heavy water is not a ‘classical’ version of light water but still presents NQEs, though to a smaller extent, as noted in a review on the topic.³⁸ This is nicely illustrated by looking at the vibrational frequencies of the O–H and O–D bond stretch mode in liquid water at ambient conditions, from which the corresponding ZPE can be estimated as ~ 21 *vs.* ~ 15 kJ/mol in light *vs.* heavy water.³⁸ Actually, the realization that the ~ 6 kJ/mol of difference in these ZPEs corresponds almost exactly to the 5.5 kJ/mol of difference between $\Delta F_{\text{H}_2\text{O}}^{\text{exp}}$ and $\Delta F_{\text{D}_2\text{O}}^{\text{exp}}$ at ambient conditions was done a long time ago.³⁶ A corollary of this observation is that, given that the present computational approach is roughly compensating for the ~ 15 kJ/mol of ZPE in heavy water, that is the same as compensating as much as a 75 % of the ZPE in light water, which helps to explain the remarkably good general performance of RPBE-D3 for H_2O .

In view of these findings, it is interesting to revisit the results of Refs. 6, 7 and 8, especially taking into account that all cases employed classical nuclei. I note in passing that the slightly different temperatures in the four cases (i.e. 298 K in Refs. 6,7 *vs.* ~ 293 K in Ref. 8 *vs.* 300 K in

this work) should imply only extremely small changes of the self-dissociation barrier in the order of ~ 0.5 kJ/mol according to the experimental data, and thus do not affect the present discussion.

I begin by noting that Joutsuka⁶ employed a O–H coordination number CV similar to the one I use here, which as I explained above introduces some energetic penalty due to the pinning of the OH⁻. Since this effect was not corrected in that work, the ΔF value of 78.2 kJ/mol found therein must be an overestimation to some extent, i.e. the correct value of the water self-dissociation barrier for revPBE-D3 would be even further below than the experimental value of 79.9 kJ/mol at 298 K. This implies that the revPBE-D3 approach used there *overcompensates* the ZPE of the O–H stretch mode in light water.

The result of Liu *et al.*⁷ can be in principle directly compared to the result in this work, considering that the CVs used there do not introduce neither the size effect nor the OH⁻ pinning effect, and moreover that the ML potential used there was trained at the same level of theory (RPBE-D3 functional) used here. However, despite these similarities, their final ΔF value is about 4 kJ/mol smaller than the value I obtained here. Since both that and the present work demonstrate an excellent convergence of the free energy barriers, it remains to be seen whether this discrepancy is due to subtle technical differences between the *ab initio* calculations underlying the training of the ML potential in that work *vs.* those used in the present work (e.g. associated to the basis sets, pseudopotentials, density cutoffs, etc), or else if it is due to the ML potential itself. On the other hand, these authors observed that explicitly including the NQEs in the simulation via path integral MD resulted in lowering the ΔF by 27.8 kJ/mol, which strongly confirms that the regular RPBE-D3 approach already compensated for most of the missing NQEs.

Finally, the result by Calegari *et al.*⁸ which is also free of both the size and pinning effects, is midway between the experimental value for H₂O and the result of this work, despite the rather different underlying *ab initio* approaches in both cases. However, in the context of the present discussion, the most interesting point of Ref. 8 is that the difference between the ΔF with and without the long range electrostatic effects amounts to more than 20 kJ/mol, while in the previous study of Liu *et al.*,⁷ the ΔF directly obtained from the FES (not accounting for the electrostatics) differs only 3.4 kJ/mol from their final value after correcting for the electrostatic effects. It is also interesting that Liu *et al.*⁷ claim that the finite-size effects in the simulation are minimal already when using a 64 H₂O cell, while Calegari *et al.*⁸ show that it is necessary to reach sizes of at least 500 H₂O molecules. Such disagreement about the actual quantitative importance of electrostatic and size effects in the water self-dissociation process is indeed intriguing, and probably merits further attention.

IV. CONCLUSIONS

In this paper, I have described a new protocol within the Blue Moon ensemble approach for estimating the free energy barrier of the self-dissociation of water in a remarkably precise way. This protocol corrects two effects present in the regular approach, which made the free energy not only quantitatively but also qualitatively wrong around the dissociated state. Such effects are: *i*) an already known finite-size effect consisting in the generated H⁺ ion causing a ‘recombination stress’ on the constrained OH⁻ as a consequence of both sharing a small simulation cell, and *ii*) a hitherto ignored localization effect due to the employed coordination number constraint, which appears whenever this constraint prohibits the diffusion of the formed OH⁻ at the dissociated state (and regardless of its precise functional form), as it happens for instance with the coordination number functions employed in Refs. 2–4,6,9.

The main advantage of this method compared to other existing approaches in the literature is that it does not require the use of very big systems, thus being affordable even at the strict *ab initio* level. This moderate computational effort makes it quite suitable for its generalized application in different situations (e.g. water at different thermodynamic conditions or environments). In particular, it could be extremely useful as a validation tool for comparing different technical approaches, from *ab initio* setups to ML potentials.

With this methodology, I obtained an estimation of the pK_w of heavy water that is almost equal to the experimental value. The comparison with the results for light water shows that there are no classical effects at all due to the different H/D masses, confirming that the origin of the different experimental pK_w values for light and heavy water is purely a nuclear quantum effect, as suggested in the literature since long ago. In addition, this result shows that the employed *ab initio* setup compensates for the NQEs in approximately the same extent as those present in heavy water, which is in turn a rather important fraction of the NQEs present in light water, in particular regarding the zero-point energy associated to the O–H bond stretch mode. This strongly supports the use of this level of theory –namely the description of the electronic structure at the RPBE-D3 level– for the study of water containing any of its two self-dissociation products, in line with the conclusions of the previous study on the diffusion of H₂O, H⁺(aq) and OH⁻(aq).¹⁸

ACKNOWLEDGMENTS

It is my pleasure to thank Sergi Ruiz-Barragan, Dominik Marx, and Jorge Kohanoff for insightful discussions. The author thankfully acknowledges the computer resources at Picasso and technical support provided by the SCBI at the Univ. of Málaga (RES-FI-2023-1-0026). This work has been supported by the Madrid Govern-

ment (Comunidad de Madrid-Spain) under the Multianual Agreement with Universidad Politécnica de Madrid in the line Support for R&D projects for Beatriz Galindo researchers, in the context of the V PRICIT (Regional Programme of Research and Technological Innovation).

- ¹B. L. Trout and M. Parrinello, *Chem. Phys. Lett.* **288**, 343 (1998).
- ²M. Sprik, *Chem. Phys.* **258**, 139 (2000).
- ³D. Muñoz-Santiburcio and D. Marx, *Phys. Rev. Lett.* **119**, 056002 (2017).
- ⁴Y. A. Perez Sirkin, A. Hassanali, and D. A. Scherlis, *J. Phys. Chem. Lett.* **9**, 5029 (2018).
- ⁵R. Wang, V. Carnevale, M. L. Klein, and E. Borguet, *J. Phys. Chem. Lett.* **11**, 54 (2020).
- ⁶T. Joutsuka, *J. Phys. Chem. B* **126**, 4565 (2022).
- ⁷L. Liu, Y. Tian, X. Yang, and C. Liu, *Phys. Rev. Lett.* **131**, 158001 (2023).
- ⁸M. C. Andrade, R. Car, and A. Selloni, *Proc. Natl. Acad. Sci. U.S.A.* **120**, e2302468120 (2023).
- ⁹S. Di Pino, Y. A. Perez Sirkin, U. N. Morzan, V. M. Sánchez, A. Hassanali, and D. A. Scherlis, *Angew. Chem. Int. Ed.* **62**, e202306526 (2023).
- ¹⁰D. Marx, *ChemPhysChem* **7**, 1848 (2006), Addendum: *ChemPhysChem* **8**, 209–210 (2007).
- ¹¹D. Marx, A. Chandra, and M. E. Tuckerman, *Chem. Rev.* **110**, 2174 (2010).
- ¹²N. Agmon, H. J. Bakker, R. K. Campen, R. H. Henchman, P. Pohl, S. Roke, M. Thämer, and A. Hassanali, *Chem. Rev.* **116**, 7642 (2016).
- ¹³E. Grifoni, G. Piccini, and M. Parrinello, *Proc. Natl. Acad. Sci. U.S.A.* **116**, 4054 (2019).
- ¹⁴(), ΔF value for H₂O dissociation computed by applying $\Delta F = pK_w RT \ln 10$ to the pK_w obtained from Eq. 39 of Ref. 15, with the H₂O density corresponding to the saturated liquid pressure at temperature T (Eq. 2.6 in Ref. 23).
- ¹⁵A. V. Bandura and S. N. Lvov, *J. Phys. Chem. Ref. Data* **35**, 15 (2006).
- ¹⁶L. Zhang, H. Wang, M. C. Muniz, A. Z. Panagiotopoulos, R. Car, *et al.*, *J. Chem. Phys.* **156** (2022).
- ¹⁷J. Sun, A. Ruzsinszky, and J. P. Perdew, *Phys. Rev. Lett.* **115**, 036402 (2015).
- ¹⁸D. Muñoz-Santiburcio, *J. Chem. Phys.* **157**, 024504 (2022).
- ¹⁹T. D. Kühne, M. Krack, F. R. Mohamed, and M. Parrinello, *Phys. Rev. Lett.* **98**, 066401 (2007).
- ²⁰T. D. Kühne, *WIREs Comput. Mol. Sci.* **4**, 391 (2014).
- ²¹G. Bussi, D. Donadio, and M. Parrinello, *J. Chem. Phys.* **126**, 014101 (2007).
- ²²T. D. Kühne, M. Iannuzzi, M. Del Ben, V. V. Rybkin, P. Seewald, F. Stein, T. Laino, R. Z. Khaliullin, O. Schütt, F. Schiffmann, D. Golze, J. Wilhelm, S. Chulkov, M. H. Bani-Hashemian, V. Weber, U. Borštnik, M. Taillefumier, A. S. Jakobovits, A. Lazaro, H. Pabst, T. Müller, R. Schade, M. Guidon, S. Andermatt, N. Holmberg, G. K. Schenter, A. Hehn, A. Bussy, F. Belleflamme, G. Tabacchi, A. Glöck, M. Lass, I. Bethune, C. J. Mundy, C. Plessl, M. Watkins, J. VandeVondele, M. Krack, and J. Hutter, *J. Chem. Phys.* **152**, 194103 (2020).
- ²³W. Wagner and A. Pruf, *J. Phys. Chem. Ref. Data* **31**, 387 (2002).
- ²⁴B. Hammer, L. B. Hansen, and J. K. Nørskov, *Phys. Rev. B* **59**, 7413 (1999).
- ²⁵S. Grimme, J. Antony, S. Ehrlich, and H. Krieg, *J. Chem. Phys.* **132**, 154104 (2010).
- ²⁶S. Goedecker, M. Teter, and J. Hutter, *Phys. Rev. B* **54**, 1703 (1996).
- ²⁷C. Hartwigsen, S. Goedecker, and J. Hutter, *Phys. Rev. B* **58**, 3641 (1998).
- ²⁸M. Krack, *Theor. Chem. Acc.* **114**, 145 (2005).
- ²⁹J. VandeVondele, M. Krack, F. Mohamed, M. Parrinello, T. Chassaing, and J. Hutter, *Comp. Phys. Comm.* **167**, 103 (2005).
- ³⁰D. Marx and J. Hutter, *Ab Initio Molecular Dynamics: Basic Theory and Advanced Methods* (Cambridge University Press, 2009).
- ³¹E. Carter, G. Ciccotti, J. T. Hynes, and R. Kapral, *Chem. Phys. Lett.* **156**, 472 (1989).
- ³²M. Sprik and G. Ciccotti, *J. Chem. Phys.* **109**, 7737 (1998).
- ³³(), the point corresponding to $\langle f_n \rangle = 0$ at $n \approx 1.965$ was interpolated from the points at $n = 1.96$ and $n = 1.97$, and introduced to avoid the cancellation error due to the changing sign of the integrand between those n values, as it is textbook knowledge.
- ³⁴A. Hassanali, M. K. Prakash, H. Eshet, and M. Parrinello, *Proc. Natl. Acad. Sci. U.S.A.* **108**, 20410 (2011).
- ³⁵(), ΔF value for D₂O dissociation computed by applying $\Delta F = pK_w RT \ln 10$ to the pK_w obtained from Eq. 7 of Ref. 36, with the D₂O density corresponding to the saturated liquid pressure at temperature T (Eq. 2 in Ref. 39).
- ³⁶R. Mesmer and D. Herting, *J. Solution Chem.* **7**, 901 (1978).
- ³⁷O. Marsalek and T. E. Markland, *J. Phys. Chem. Lett.* **8**, 1545 (2017).
- ³⁸M. Ceriotti, W. Fang, P. G. Kusalik, R. H. McKenzie, A. Michaelides, M. A. Morales, and T. E. Markland, *Chem. Rev.* **116**, 7529 (2016).
- ³⁹S. Herrig, M. Thol, A. H. Harvey, and E. W. Lemmon, *J. Phys. Chem. Ref. Data* **47**, 043102 (2018).